Available online at www.sciencedirect.com
ScienceDirect
Ceramics International 34 (2008) 2059–2066
CERAMICS INTERNATIONAL
www.elsevier.com/locate/ceramint

Effect of the drying techniques on the morphology of silica nanoparticles synthesized via sol–gel process

I.A. Rahman [a,*], P. Vejayakumaran [a], C.S. Sipaut [a], J. Ismail [a], C.K. Chee [b]

[a] School of Chemical Sciences, Universiti Sains Malaysia, 11800 Penang, Malaysia
[b] Intel Technology (M) Sdn Bhd, Bayan Lepas FTZ Phase III, 11900 Penang, Malaysia

Received 1 June 2007; received in revised form 4 July 2007; accepted 2 August 2007
Available online 2 October 2007

Abstract

The effect of drying techniques on the dispersion and agglomeration of silica nanoparticles were studied using alcohol-dehydration (AD), freeze-drying (FD) and oven drying (OD) techniques. Observation under optical microscope showed that aqueous-dispersion with OD technique led to the formation of densely packed particles (islands) while AD resulted in loosely packed particles with non-isotropic aggregation pattern. TEM analysis showed that most of the silica nanoparticles were homogenous and discrete in nature. The comparison between experimental (S_{BET}) and theoretical ($S_{spherical}$) surface area indicated that the agglomeration of nanoparticles increased in the order of AD < FD < OD. The decrease in the silanol number in the order of AD > FD > OD and the increase in the pore size (D_p) and pore volume (V_p) in the order of AD < FD < OD further supports the agglomeration trend predicted by the surface area comparison. The results suggested that agglomeration can be effectively reduced by eliminating water from the system before solidification since the presence of water during the process could intense the interparticle interactions leading to agglomeration. Overall a new, simple and cost effective drying technique (AD) has been developed to produce silica nanoparticles with improved dispersion and reduced agglomeration.

Keywords: Silica nanoparticles; Sol–gel; Alcohol-dehydration; Morphology

1. Introduction

Advancement in nanotechnology has led to the production of nano-size silica through sol–gel process which has been widely used in both scientific research and engineering development [1]. Stöber synthesis [2] which involves ammonia-catalyzed reactions of tetraethylorthosilicate (TEOS) with water in low molecular weight alcohol has been used as a platform to synthesize silica nanoparticles with various characteristics. Optimizing the reaction conditions [3,4], addition of ionic additives [5,6] and microemulsion techniques [7,8] were some of the recent attempts made by the scientists to reduce the silica size using the Stöber synthesis as a platform.

Dispersion and agglomeration of silica nanoparticles are two essential factors that govern its application prospect in the preparation of advance nanocomposites [1,9]. Production of highly dispersive nanoparticles (e.g. primary silica particles below 10 nm) with low agglomeration level in powder form is still a challenge owing to the fact that these particles were highly sensitive to the processing conditions [10]. In the preparation of silica-polymer nanocomposite, the presence of agglomerates can significantly increase the viscosity of the matrix which leads to difficulty in dispensing the matrix [1]. In addition to that, the agglomerates also can reduce the silica loading, resulting in reduced thermomechanical properties [11].

Collision and coalescence of the nanoparticles are main factors that govern the extent of agglomeration in a nanoparticles powder system. Besides high temperature coalescence, the liquid-to-solid transition during the drying process of a colloid can be destructive to the morphology of the constituting nanoparticles since it involves major phase transition. Drying is a simple process which involves fluid to solid transition leading to the formation of solid materials. The drying techniques used to discard water from a colloid system can be divided into two main categories: thermal and non-thermal. Oven and spray drying, for example, falls in the former category while freeze-drying, desiccation with silica gel and

* Corresponding author. Tel.: +60 4 6533262; fax: +60 4 6574854.
E-mail address: arismail@usm.my (I.A. Rahman).

0272-8842/$34.00
doi:10.1016/j.ceramint.2007.08.014

chemical extraction of the solvent falls in the latter category. The hydrodynamic effect [12], van der Waals forces and Brownian motions can lead to a complex agglomeration behavior in a typical drying process [10].

In our previous work [4], we developed an effective method to produce silica nanoparticles in their primary size range by optimizing the experimental conditions of the sol–gel process. The work mainly focused on reducing the silica size in the nano-range. In this continuation work, we focused on the processing conditions of the freshly synthesized silica. In this paper, we described the effect of drying techniques on the morphology (size, size distribution, dispersion and agglomeration) of silica nanoparticles produced via sol–gel process. Silica nanoparticles in their primary size range were selected for the study since these particles exhibit prominent interparticle forces [10].

Three different types of drying techniques were employed in this study to remove the water, namely oven drying (thermal method), freeze-drying (non-thermal method) and alcohol-dehydration (chemical extraction method). Macroscopic drying patterns of the silica nanoparticles under various drying conditions have provided some useful insights on the particle–particle interactions during the drying process. In addition to that, BET surface area, pore size, pore volume, pore volume distribution and silanol distributions has been used to evaluate the extent of agglomeration in each samples. Some possible chemical reactions which can lead to the agglomeration during the agitation and drying process have been discussed as well.

2. Experimental

2.1. Synthesis and processing of freshly synthesized silica nanoparticles

Silica nanoparticles were synthesized by the hydrolysis and condensation of tetraethylorthosilicate, TEOS (99.9%, Fluka) in absolute ethanol (EtOH 99.5%, Systerm) containing distilled water and ammonia as base catalyst (NH_3 25%, Merck). The optimal experimental conditions and procedure for the synthesis was taken from our previous work [4]. The resulting transparent 'fragile gel' was dispersed into EtOH, washed (to remove the unreacted reactant and excess catalyst) and dried, crushed and calcined at 500 °C (to remove organic impurities) prior to the characterizations. The following section describes the different washing and drying techniques used in this study.

2.1.1. Oven drying (OD)

The fragile gel form was first stirred in EtOH (20 wt% EtOH) to disperse the nanoparticles. Then, the particles were separated from the solution phase using centrifuge machine (Kubota Corporation, model 5920) operated at 5000 rpm/10 min. The separated particles were dispersed and washed thoroughly with distilled water (20 wt% H_2O) through agitation using magnetic stirrer and followed by centrifugal separation. The cycle was repeated for three times and the final product was made into water suspension and dried in conventional drying oven at 80 °C for 24 h.

2.1.2. Freeze-drying (FD)

The washing procedure was exactly the same as described above. In this technique, the final suspension of silica (colloid) was frozen at 0 °C and the resulting solid was freeze-dried using Labconco FreeZone® 12 Liter Freeze Dry System for 24 h.

2.1.3. Alcohol-dehydration (AD) technique

In this technique, the freshly synthesized silica was dispersed using series of medium prepared at different ratios of EtOH:H_2O (1:1, 3:2, 1:0, 1:0 and 1:0) at 20 wt% of the medium. Each agitation was followed by centrifugal separation as described in Section 2.1.1. After the fifth agitation, the separated particle were made into alcohol suspension and dried at 70 °C for 3 h in conventional drying oven (to discard the alcohol).

2.2. Characterizations

The moisture content of the silica samples was determined using the following procedure. Approximately 2 g of silica was weighed into a weighing bottle (which was first dried at 105 °C) and dried for 2 h in a conventional drying oven at 105 °C. After cooling in desiccator, the loss of weight was measured by calculating the difference between the sample weight before and after drying.

Perkin-Elmer 2000 FTIR Spectrometer was used to analyze the contents of the supernatants collected from the centrifugal separation. The liquid samples were dropped onto the ZnSe crystals and spread to form a thin layer followed by scanning in the range of 4000–650 cm^{-1}.

Optical micrographs of the dried silica suspensions were taken using Nikon Ellispe E600 light microscope. The samples were prepared by dropping the respective final suspensions (after washing) onto glass slits and drying according to the prescribed conditions in Section 2.1.

A Philips CM12 transmission electron microscope (TEM) was used to analyze the morphology of the processed nanoparticles at an accelerating voltage of 80 kV. The processed samples (washed, dried, ground and calcined) were dispersed in ethanol and placed on copper grids covered with carbon coating for the TEM observation. The average particle size (average diameter), D and statistical parameters were determined based on the measurement of more than 300 particles from the TEM micrographs using analySIS Docu Version 3.2 image processing software.

Surface area and porosity measurements were obtained using nitrogen adsorption–desorption (77 K) and the Brunauer–Emmett–Teller (BET) algorithm on a Micromeritics ASAP 2000 adsorption analyzer. The samples were degassed at 105 °C for overnight under vacuum (10^{-3} mmHg). The specific surface area, S_{BET} was obtained using BET equation while the total pore volume, V_p, was estimated from the amount of nitrogen adsorbed at relative pressure ≈0.98–0.99 using Kelvin's equation [13]. The pore size distributions was calculated based on desorption curve of the isotherm by Barret–Joyner–Halenda (BJH) method.

Assuming the silica particles to be homogenous, nonporous and spherical in shape, theoretical surface area of the nanoparticles in $m^2\ g^{-1}$ was calculated using spherical model using the following equation [13,14]:

$$S_{\text{spherical}} = \frac{6}{\rho D} \quad (1)$$

in which ρ is the density (assumed to be $2.0 \times 10^6\ g\ m^{-3}$, a typical average density of silica prepared via wet-synthesis conditions [15]) and D is the average particle diameter in m.

Concentration of silanol groups per unit grams of silica samples (δ_{OH}) was estimated using alkali neutralization method as been described in the literature [16,17]. Silanol number, α_{OH} which refers to the number of hydroxyl groups per nm^2 of silica surface was calculated using the following formulation [14]:

$$\alpha_{OH} = \delta_{OH} N_A 10^{-21} S^{-1} \quad (2)$$

in which δ_{OH} is the concentration of the silanol groups (mmol g^{-1}), N_A the Avogadro number and S is the specific surface area.

3. Results and discussion

3.1. Efficiency of alcohol-dehydration (AD) technique

The efficiency of alcohol-dehydration was investigated by determining the moisture (free H_2O) content of the samples after each steps of agitation and the results were shown in Table 1. The result indicated that the water molecules were successfully extracted out from the silica samples especially after the fourth agitation with the moisture content reduced to ~1.1 wt% SiO_2. The water content of the final products (before calcination) prepared using the FD and OD techniques was 2.3 and 0.9 wt% SiO_2, respectively (Table 2). Higher water content showed by the FD technique is due to the water molecules trapped [18] between the closely packed nanoparticles. The results showed that the AD technique effectively removed the water molecules at shorter time and lower temperature if compared to the OD technique. The method is also cost effective since the EtOH used can be easily recycled and reused using distillation process.

Table 1
Water content in the silica samples after various levels of washing in the alcohol-dehydration (AD) technique

Step	EtOH:H_2O (v/v)	H_2O content (wt%)
1	1:1	5.57 ± 0.38
2	3:2	2.89 ± 0.21
3	1:0	1.82 ± 0.12
4	1:0	1.06 ± 0.09
5	1:0	1.10 ± 0.07

The FTIR analysis (Fig. 1) showed that the AD technique is also effective in removing the excess reactants from the system. As shown in the figure the peaks corresponding to TEOS, i.e. 1169.69 cm^{-1} (Si–O–Si, skeleton (overtone) vibrations) and 966.07 cm^{-1} (Si–O–(H···H_2O), bending vibration) [14] was observed in the first wash but disappeared in the fifth wash (the spectrum was identical to pure EtOH), indicating the removal process was successful. In addition to that, the disappearance of peak at 1644.37 cm^{-1} (bending O–H (molecular water) [14]) in the same manner further confirmed the efficiency of AD technique in discarding water from the silica samples.

3.2. Drying patterns

Drying pattern can provide useful information regarding interparticle interactions during the drying process. As shown in Fig. 2(a), the OD technique leads to the formation of dense islands (consist of closely packed particles). The emergence of meniscus boundary between islands indicates that a strong capillary force has been created during the drying process [19]. The process can be explained as follows. During the drying process, the water molecules were constantly eliminated. The elimination of water molecules during the process caused the concentration of the sol to increase and also created fluid drag, which caused the particles to come closer to each other. At a

Table 2
Structural and physical properties of the primary silica prepared using different drying techniques

Structural properties of the primary silica	Drying techniques		
	Alcohol-dehydration (AD)	Freeze-drying (FD)	Oven drying (OD)
Average particle diameter, D (nm)	6.7 ± 1.6	6.9 ± 1.7	7.1 ± 1.8
BET surface area, S_{BET} ($m^2\ g^{-1}$)	480 ± 3.9	378 ± 3.6	343 ± 3.4
Theoretical surface area, $S_{spherical}$ ($m^2\ g^{-1}$)[a]	446 (23.9)	432 (24.6)	423 (25.5)
R_s (ratio of $S_{BET}/S_{spherical}$)[b]	1.08	0.88	0.81
Pore diameter, D_p (nm)	6.9 ± 0.4	8.9 ± 0.9	18.2 ± 3.2
Total pore volume, V_p ($cm^3\ g^{-1}$)	0.782 ± 0.014	0.783 ± 0.009	1.711 ± 0.022
Micropore volume, V_{mp} ($cm^3\ g^{-1}$)	0	0.015 ± 0.0001	0.012 ± 0.0001
Silanol concentration, δ_{OH} (mmol g^{-1})[c]	2.589 ± 0.12	1.864 ± 0.08	1.453 ± 0.07
Silanol number, α_{OH} (OH nm^{-2})	3.25	2.97	2.55
Moisture content (%)	1.12 ± 0.07	2.33 ± 0.18	0.92 ± 0.08
Weight loss after calcination (%)[d]	5.15 ± 0.28	5.32 ± 0.32	4.94 ± 0.36

[a] Surface area calculated based on spherical model.
[b] Represent the ratio between the experimental values with the theoretical values. Values in the brackets refer to the error (%).
[c] Silanol concentrations of the calcined samples (500 °C/2 h).
[d] Values refer to the total loss in the 105–500 °C temperature range.

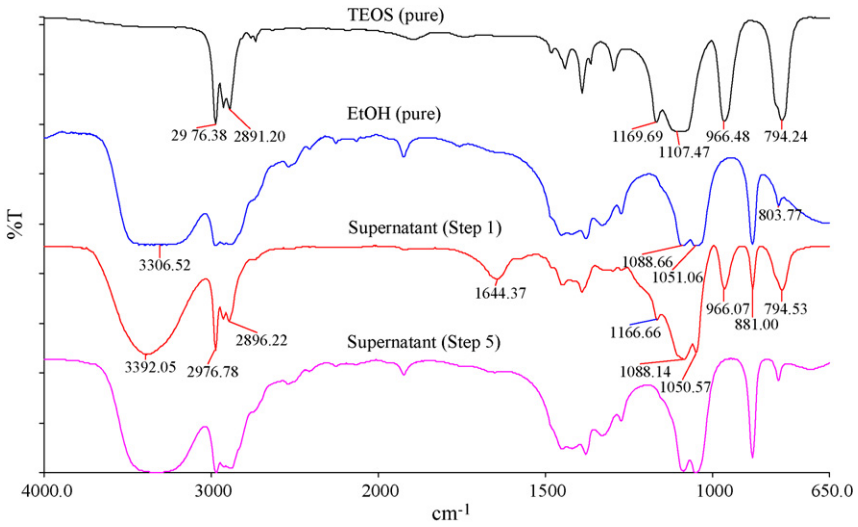

Fig. 1. FTIR spectrums of the supernatants (liquid) collected after first and fifth agitation of primary silica using alcohol-dehydration technique as compared to the spectrums of pure TEOS and EtOH.

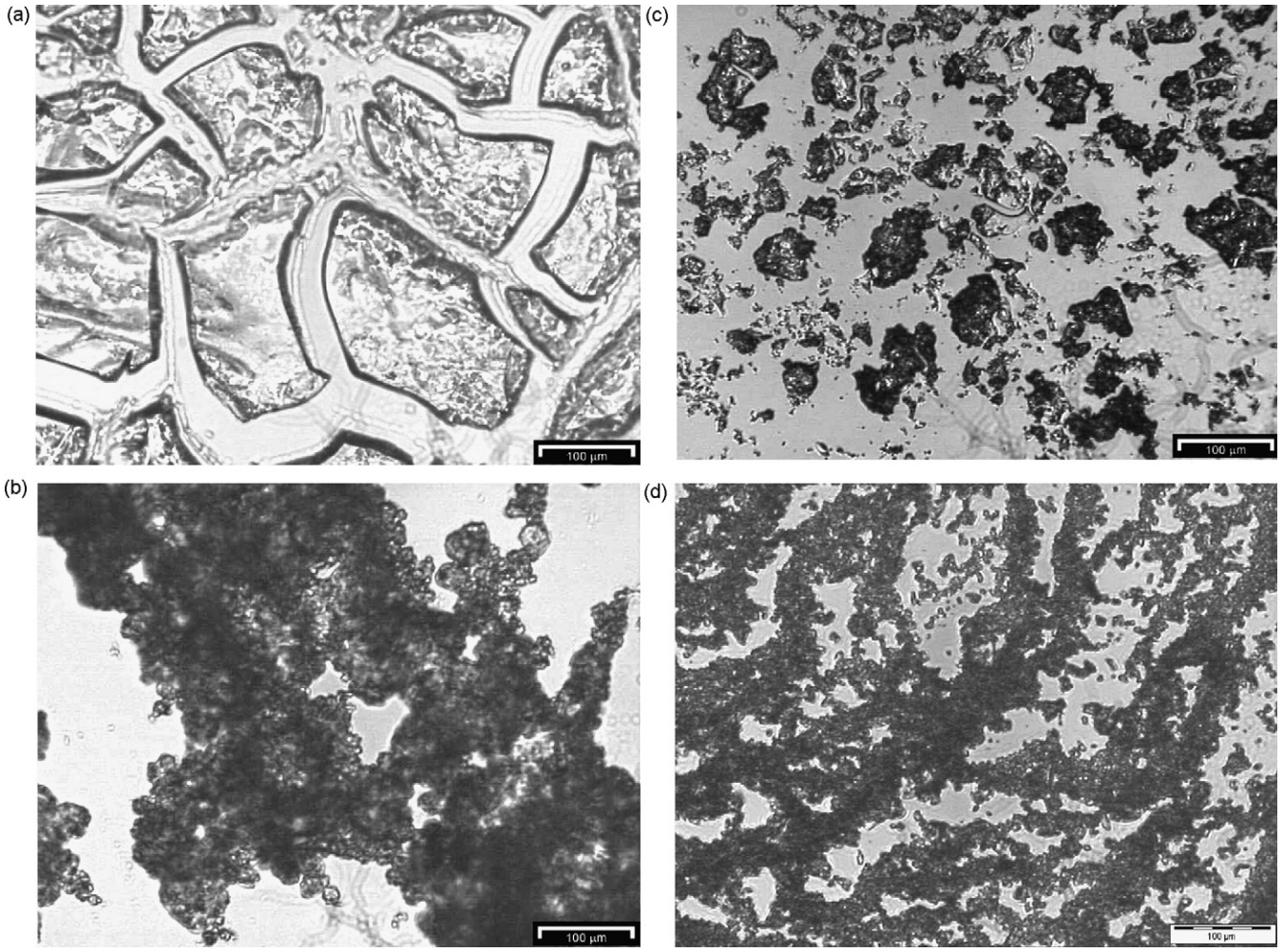

Fig. 2. Drying patterns of the freshly synthesized primary silica observed under optical microscope after (a) OD, (b) FD, (c) AD and (d) typical drying pattern of the suspension containing processed powder at 2 wt% H_2O.

critical point, these particles touch each other and forms aggregate to achieve greater stability. Hydrogen bonding (through silanol groups), van der Waals and capillary forces were the dominant attraction forces acting on these nanoparticles [10,20]. The voids and microcracks observed on the islands were created by the evaporation of physically adsorbed water from the surface. We believe that thermophoresis and microcirculation phenomena as suggested by Iskandar et al. [12] were responsible for the reorganization of the nanoparticles leading to the formation of well-defined islands.

In contrast to the OD technique, FD showed a bulk aggregation pattern consisting of loosely packed particles (Fig. 2(b)). In the FD technique the liquid phase was completely avoided since it involves solid–gas transition. Thus capillary force which can lead to the compaction of particles was avoided. The bright fields observed in the image refer to the loosely compacted particles. The volume expansion occurred during the freezing of the aqueous suspension (ice formation) also could contribute to the loose packing. On the other hand, the AD technique showed a non-isotropic (not homogenous) aggregation pattern (Fig. 2(c)). The size of the aggregates was significantly smaller than FD, i.e. ~70 μm. Besides the bulk aggregates, the presence of fine aggregates with average size of ~2 μm was also observed. This indicates that the AD technique significantly reduced the particle–particle contact during the drying process compared to other techniques. This is due to the effective removal of water from the system (Table 1). The elimination of water avoids the bridging phenomena between the particles [9] thus reducing the particle–particle contact. Besides that, EtOH could form hydrogen bonding with the silanol groups and reduce the hydrophilic behavior of the silica surface. Low surface tension (23 mN m^{-1} at 20 °C [21]) and boiling point (78 °C) of EtOH makes it easily evaporated from the sol system as compared to water (surface tension = 73 mN m^{-1} at 20 °C [21]). The lower surface tension of EtOH also avoids the capillary drag during the drying process, leading to loose packing of the nanoparticles.

These results showed that OD technique results in an enhanced interparticle interaction compared to FD and AD techniques. The drying pattern of the processed powder (Fig. 2(d)) showed that the particles were present in the form of soft aggregates in granular forms. Same pattern was observed for all samples regardless of the drying techniques (OD, FD and AD). This observation indicates that the particles were stabilized after the processing [22] and the first drying is the most important step that controls the interparticle interaction. The results also showed that the presence of liquid water during the drying process can increase the particle–particle interaction during the drying process.

3.3. Morphology of silica nanoparticles under different drying conditions

The discrete nanoparticles were not really spherical in shape, as it was reported previously [4]. Despite showing insignificant difference in the dispersion and particle shape, the average size of the nanoparticles was differed slightly as shown in Table 2. The particle size (of the measurable discrete particles) increased in the order of AD < FD < OD. All the samples showed a narrow size distribution (Fig. 3). However, as shown in the figure, the frequency of the particles above ~7 nm increased in the order of AD < FD < OD. In addition to the discrete particles few types of agglomerate was observed in the samples (Fig. 4). Type 1 exhibited relatively dense structure consisting of strongly fused particles [20]. On the other hand, Type 2 showed a fractal structure (polymeric clusters) [20] while Type 3 was the smallest agglomerate observed. The probability, P of finding each type of these agglomerates is given in Table 3. The results showed that Type 1 and Type 2 was the highest in OD samples followed by FD and AD, respectively. There was no significant increase in the probability of Type 1 and 2 agglomerates after the calcination except for Type 3 agglomerate (increased from P = ~0.1 to P = ~0.3). The weight loss of the samples after the calcination process was found to be almost constant at ~5% (Table 2). This weight loss is due to the dehydroxylation (removal of silanol groups) process which results in the formation of new siloxane bonds [14,20] which could mainly contribute to the formation of Type 3 agglomerates. In general, OD showed high degree of agglomeration compared to other techniques.

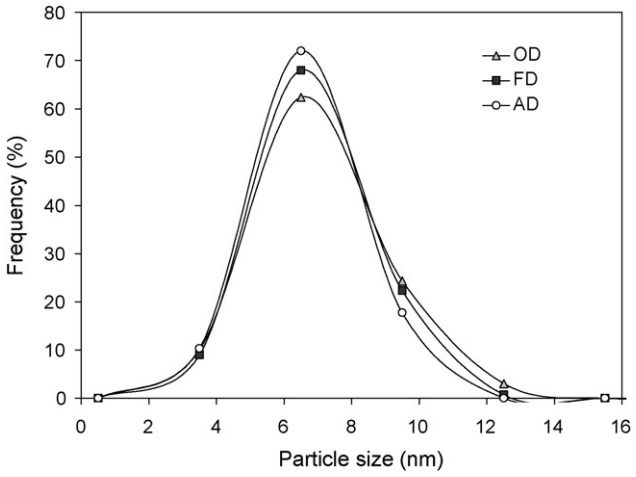

Fig. 3. Size distribution of the silica nanoparticles prepared via different drying techniques.

3.4. Surface and pore analysis

N_2 adsorption study was conducted to investigate the characteristics of the nanopowder in the solid state. As shown in Table 2, S_{BET} increased in the order of OD < FD < AD which correlates with the trend showed by the theoretical surface area, $S_{spherical}$. Although in the real case the particles were not really spherical in shape, the spherical model still can be used to get some insights on the dispersion and agglomeration behavior of the nanoparticles. The agglomeration phenomena can readily reduce the surface area since the nanoparticles will fuse together to form a bulk structure, which is bigger than the discrete particles [20]. Smaller R_s value showed by the OD sample (~0.8) compared to FD (~0.9) suggest that the agglomeration was higher in the OD sample (Table 2). However

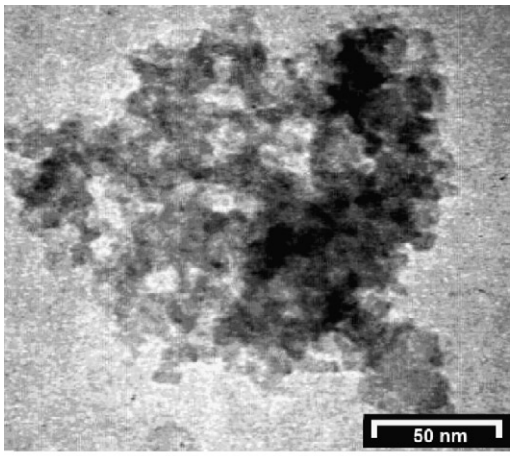

Type 1(141.6 nm)

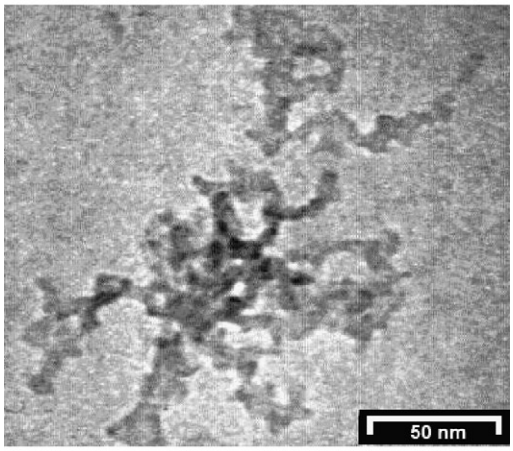

Type 2 (135. 5 nm)

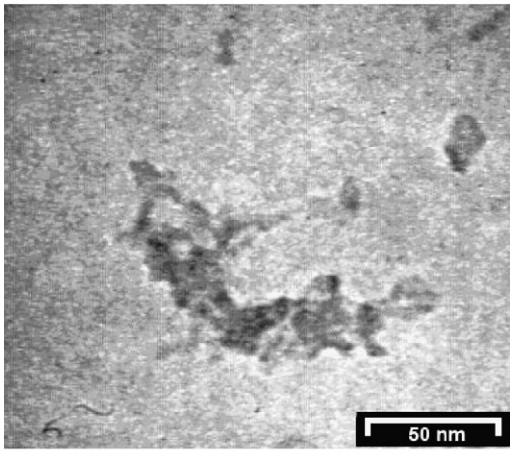

Type 3 (32.2 nm)

Fig. 4. Note: The average size of types of agglomerates found in the samples prepared via different drying techniques.

for AD sample the R_s value was found greater than 1. This is due to high standard deviation of the average particle size (D) which increased the error of the theoretical calculation (Eq. (1)). Nevertheless, the experimental value still fell within the upper limit of the theoretical value which is 551 $m^2\ g^{-1}$. These results suggested that more than 80% of the silica nanoparticles (regardless of the drying techniques) were present in discrete

Table 3
Probability of finding the Type 1, Type 2 and Type 3 agglomerates in the silica samples prepared via different drying techniques

Agglomerate	Probability (P)					
	Before calcination			After calcination		
	OD	FD	AD	OD	FD	AD
Type 1	0.27	0.10	0.04	0.28	0.12	0.05
Type 2	0.21	0.13	0.08	0.23	0.13	0.10
Type 3	0.12	0.13	0.10	0.32	0.31	0.33

Note: The probability, P of finding these agglomerates in each sample was calculated based on number of agglomerates observed per 300 discrete particles from randomly selected TEM images using the following equation: P = no. of agglomerate/no. of discrete particles.

form. Silanol number, α_{OH} was calculated to confirm the results predicted above. As given in Table 2, the silanol number decreased in the order of AD > FD > OD. The decrease in the silanol number suggested that the silanol groups have reacted to form siloxane bond during the agglomeration process, with the OD samples showing the highest agglomeration reactions, followed by FD and AD samples, respectively.

The N_2/77 K adsorption–desorption isotherms of the nanoparticles prepared via different drying techniques are given in Fig. 5(a). All isotherms belong to the Type IV of the Brunauer–Deming–Deming–Emmett classifications, typical of mesoporous material [23]. Since the majority of the particles are present in the discrete form (TEM analysis), the porosity was mainly caused by the compaction of the nanoparticles [13] due to enhanced van der Waals attraction [10,20]. As shown in the figure the relative pressure at which capillary condensation occurred increased from AD to OD, indicating the increase in the pore size. Correlating to this, the D_p and V_p was found increased in the order of AD < FD < OD (Table 2). The pore size distribution (Fig. 5(b)) was found shifted to higher D_p value in the same order. The pores were created by the voids present between the nanoparticles, between the nanoparticles and agglomerates and also within (see Fig. 4) and between the agglomerates [13]. The high pore size and volume showed by the OD samples indicate the presence of open structures due to agglomeration [13]. These open structures results in loose packing of the nanoparticles. Interestingly, no micropores were detected on the AD samples. FD and OD samples showed the presence of micropores, which could be the fine pores present within the agglomerates. All the samples showed a H1 hysteresis loop, typical for agglomerates or compacts of spherical particles with homogenous size and array [13]. These findings strongly suggests that the agglomeration increased in the order of AD < FD < OD.

3.5. Reactions leading to the agglomeration of silica nanoparticles at low temperature

The differences in the particle size, size distributions and agglomeration levels as discussed above were mainly due to the drying technique used since all the other processing conditions (synthesis condition, grinding and calcination) were fixed and

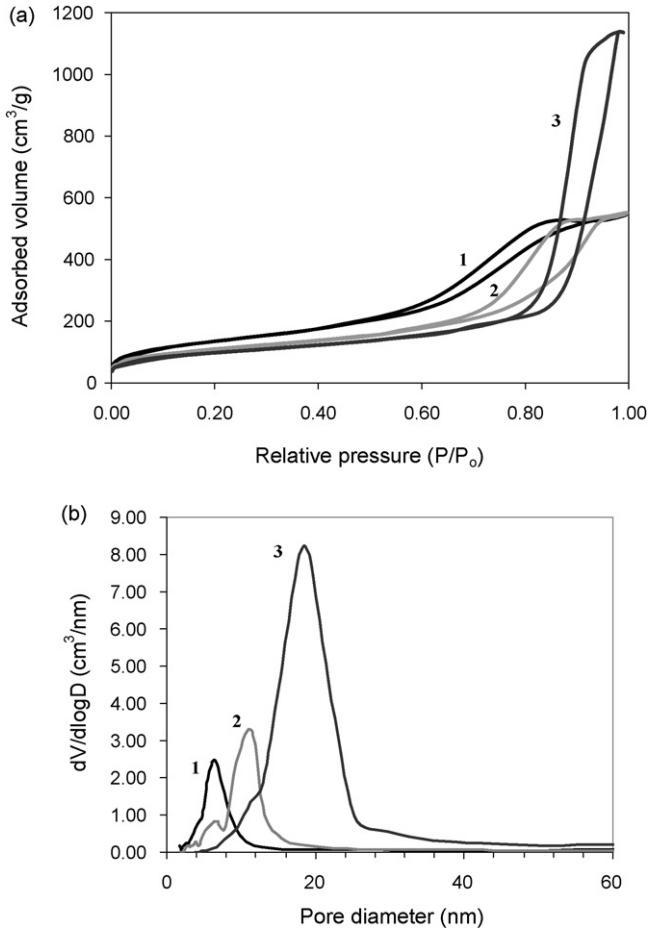

Fig. 5. (a) Nitrogen adsorption–desorption isotherms and (b) pore size distribution for primary silica particles prepared using different drying techniques, i.e. (1) AD, (2) FD and (3) OD.

standardized. The phenomena can be explained by analyzing the agitation and drying process and some possible chemical reactions that might occur at the silica–silica interface. The following equation describes the main chemical reaction involved in the formation of agglomerates in silica powder:

$$\equiv Si{-}OH + HO{-}Si\equiv \rightarrow \equiv Si{-}O{-}Si\equiv + H_2O \quad (3)$$

As discussed in Section 3.2, the interparticle interaction was highest in the OD technique. The Brownian motion, hydrodynamic effect and capillary drag has leaded the nanoparticles to collide readily and the inelastic collisions resulted in the formation of agglomerates [10]. Boyle et al. [9] has suggested that the water molecules present in the form of bridges between the nanoparticles can reinforce the agglomeration cohesivity. This possibility has been effectively avoided in AD technique by removing the water molecules from the sol system. The slight increase in the size of the nanoparticles is possibly due to the fact that small amount of nanoparticles can dissolve (reverse of Eq. (3)) and reprecipitate on the existing nanoparticles, as suggested by Kwon and Messing [10]. Besides them, Brinker [20] also reported that the solubility of particles can increase as the particle size reduced into nanoscale especially at elevated temperature. Besides increasing the particle size, the phenomena also can cause agglomeration and necking between the boehmite nanoparticles [10]. This is also possible in our case since the nanoparticles were repeatedly agitated in water prior to the drying process in both OD and FD techniques. The possibility of dissolution and reprecipitation is even higher in OD since the aqueous sol was heated at 80 °C during the drying process. In addition to that, Ma et al. [24] has demonstrated the possibilities of hydrolysis and clustering on various characteristic defect sites on the silica surface using molecular dynamics simulation. Thus, clustering phenomena at defected sites (e.g. dangling oxygen atom, ≡Si–O) of the silica surface also could contribute to the formation of agglomerates in the aqueous systems (for OD and FD). It can be seen that water is playing an important role in promoting all these reactions. Hence, the AD technique was effective in increasing the dispersion and reducing the agglomeration of silica nanoparticles since it was able to control all the possible agglomeration reactions by merely eliminating water from the particles before it solidifies.

4. Conclusions

We have studied the effect of various drying techniques (thermal, non-thermal and chemical extraction) on the morphology of silica nanoparticles synthesized via sol–gel process. The AD technique has effectively removed the water and excess reactants from the silica suspension. Macroscopic drying pattern showed that the OD technique leads to the formation of dense islands due to intense interparticle interactions and capillary force created by the evaporating water. In contrast, both FD and AD techniques lead to the formation of aggregates which were loosely packed. The TEM analysis indicated that majority of the particles were discrete and monodispersed. The analysis also revealed the presence of agglomerates, which was highest in the OD samples and least in the AD samples. The S_{BET} increased in the order of OD < FD < AD. The R_s value increased in the same order, indicating a decrease in the degree of agglomeration. The results were further supported by the silanol number which was increased in the similar order. All the samples exhibited mesoporous behavior. The presence of open structures (agglomerates) resulted in increased D_p and V_p values due to reduced compaction of the nanoparticles. Highest D_p and V_p values were observed for the OD samples. Inelastic collisions due to hydrodynamic effect and Brownian motion, dissolution and reprecipitation of the nanoparticles and clustering phenomena at defected sites of the silica surface has been suggested to promote agglomeration at low temperature. In conclusion, AD technique produced highly discrete particles with a very low degree of agglomeration, opposite to the OD technique while FD showed moderate effects on the properties of interest.

Acknowledgments

The authors would like to thank Intel Technology (M) Sdn. Bhd. for financing this research through grant nos. 304/PKIMIA/650392/I104 and 304/PKIMIA/650336/I104. We also

thank Mr. Pachamuthu (EM unit) for his contributions in developing the alcohol-dehydration technique.

References

[1] Y. Sun, Z. Zhang, C.P. Wong, Study on mono-dispersed nano-size silica by surface modification for underfill applications, J. Colloid Interface Sci. 292 (2005) 436–444.
[2] W. Stöber, A. Fink, E. Bohn, Controlled growth of monodisperse silica spheres in the micron size range, J. Colloid Interface Sci. 26 (1968) 62.
[3] S.K. Park, K.D. Kim, H.T. Kim, Preparation of silica nanoparticles: determination of the optimal synthesis conditions for small and uniform particles, Colloids Surf. A 197 (2002) 7–17.
[4] I.A. Rahman, P. Vejayakumaran, C.S. Sipaut, J. Ismail, M. Abu Bakar, R. Adnan, C.K. Chee, An optimized sol–gel synthesis of stable primary equivalent silica particles, Colloids Surf. A 294 (2007) 102–110.
[5] S.S. Kim, H.S. Kim, S.G. Kim, W.S. Kim, Effect of electrolyte additives on sol-precipitated nano silica particles, Ceram. Int. 30 (2004) 171–175.
[6] I.A. Rahman, P. Vejayakumaran, C.S. Sipaut, J. Ismail, M. Abu Bakar, R. Adnan, C.K. Chee, The effect of anion electrolytes on the formation of silica nanoparticles via sol–gel process, Ceram. Int. 32 (2006) 691–699.
[7] F.J. Arriagada, K. Osseo-Asare, Synthesis of nanosize silica in a nonionic water-in-oil microemulsion: effects of the water/surfactant molar ratio and ammonia concentration, J. Colloid Interface Sci. 211 (1999) 210–220.
[8] P.R. Kust, R.A. Hendel, M.A. Markowitz, P.E. Schoen, B.P. Gaber, Effect of surfactant and oil type on the solution synthesis of nanosized silica, Colloids Surf. A 168 (2000) 207–214.
[9] J.F. Boyle, I. Manas-Zloczower, D.L. Feke, Hydrodynamic analysis of the mechanisms of agglomerate dispersion, Powder Technol. 153 (2005) 127–133.
[10] S. Kwon, G.L. Messing, The effect of particle solubility on the strength of nanocrystalline agglomerates: Boehmite, Nanostruct. Mater. 8 (1997) 399–418.
[11] A.V. Shenoy, Rheology of Filled Polymer Systems, Kluwer Academic, Dortdrecht, 1999.
[12] F. Iskandar, L. Gradon, K. Okuyama, Control of the morphology of nanostructured particles prepared by the spray drying of a nanoparticle sol, J. Colloid Interface Sci. 265 (2003) 296–303.
[13] S.J. Gregg, K.S.W. Sing, Adsorption, Surface Area and Porosity, 2nd ed., Academic Press, London, 1982.
[14] E.F. Vansant, P. Van Der Voort, K.C. Vrancken, Characterization and Chemical Modification of the Silica Surface, Elsevier Science, New York, 1995.
[15] G. Michael, H. Ferch, Schriftenreihe Pigmente, Degussa 11 (1991).
[16] S. Yuaga, M. Okabayahi, H. Ohno, K. Suzuki, K. Kusumoto, Amorphous, spherical inorganic compound and process for preparation thereof, US Patent 4,764,497 (1988).
[17] S. Kang, S.H. Sung, C.R. Choe, M. Park, S. Rim, J. Kim, Preparation and characterization of epoxy composites filled with functionalized nanosilica particles obtained via sol–gel process, Polymer 42 (2001) 879–887.
[18] A.B. Bashaiwoldu, F. Podczeck, J.M. Newton, A study on the effect of drying techniques on the mechanical properties of pellets and compacted pellets, Eur. J. Pharm. Sci. 21 (2004) 119–129.
[19] H. Komiyama, Y. Yamaguchi, S. Noda, Structuring knowledge on nano-materials processing, Chem. Eng. Sci. 59 (2004) 5085–5090.
[20] C.J. Brinker, G.W. Scherer, Sol–Gel Science: The Physics and Chemistry of Sol–Gel Processing, Academic Press Inc., San Diego, 1990.
[21] J.S. Reed, Principles of Ceramics Processing, 2nd ed., Wiley–Interscience Publication, New York, 1995.
[22] D. Barby, in: G.D. Parfitt, G.S.W. Sing (Eds.), Silicas Characterization of Powder Surfaces, Academic Press, London, 1976.
[23] S. Brunaeur, P.H. Emmet, E. Teller, Adsorption of gases in multimolecular layers, J. Am. Chem. Soc. 60 (1938) 309–319.
[24] Y. Ma, A.S. Foster, R.M. Nieminen, Reactions and clustering of water with silica surface, J. Chem. Phys. 122 (2005) 144709.